nature physics

Review article

https://doi.org/10.1038/s41567-025-02994-7

Accelerator technologies for proton and ion beam therapy

Received: 5 May 2024

Accepted: 8 July 2025

Published online: 3 September 2025

Check for updates

Vivek Maradia[1,2] ✉, Benjamin Clasie[3], Emma Snively[4], Katia Parodi[5], Marco Schwarz[6,7] & Marco Durante[8,9,10]

Over the past 75 years, proton beam therapy has emerged as a promising modality for cancer treatment, boasting precise targeting and reduced collateral damage to healthy tissue. Here we discuss the evolution of accelerator technology in proton therapy, examining advancements in cyclotron, synchrotron and linear accelerator technology, and their implications for modern treatment delivery. Additionally, we explore advances in delivering accelerated carbon or helium ions for therapeutic treatments. We also discuss the integration of advanced imaging modalities, such as multienergy X-ray, magnetic resonance imaging and ion-based imaging, for real-time monitoring and adaptive radiotherapy. These advancements position particle therapy to offer personalized and effective cancer treatment strategies, heralding improved patient outcomes.

Cancer treatment typically involves several options (Table 1), including surgery, chemotherapy and radiotherapy—the use of high-energy radiation to destroy cancer cells. Conventional radiotherapy, such as X-ray (photon) therapy, is widely used to treat many types of cancer. However, its limitation lies in the fact that photons deposit energy along their entire path, which can result in damage to surrounding healthy tissues, particularly for tumours located near critical organs, such as brain, lungs, liver, heart and spinal cord.

Proton therapy represents a promising approach in cancer treatment, offering precise localization of radiation dosage. Protons exhibit a characteristic peak in energy deposition within tissue known as the Bragg peak[1]. In proton therapy, the dose is delivered by overlapping individual Bragg peaks through successive beam energy adjustments tailored to the tumour size and location, producing precise and uniform dose distributions. Compared with the spread-out Bragg peak, the depth-dose distribution of a large 10-MV photon field shows a substantial variation in dose deposition outside the target, as can be seen in Fig. 1. The two red-shaded areas highlight that photon radiation delivers a 2.2 times higher dose to the surrounding healthy brain tissue than proton radiation in this scenario, which involves a tumour near the brainstem. For protons, the only higher doses occur at the skin and entry points, indicated by the blue-shaded area. A metric for comparing the biological effectiveness of various radiation types is the so-called relative biological effectiveness. It is defined as the relative ability of a specific type of radiation to cause biological damage compared with a reference radiation—usually X-rays or gamma rays. For protons, this measure is typically 1.1, suggesting that protons are approximately 10% more effective at inducing biological damage than conventional X-rays.

Emerging evidence suggests potential clinical advantages of proton therapy, particularly in mitigating acute toxicities in head-and-neck cancer treatment and reducing late effects in paediatric brain tumour treatment[2,3]. Furthermore, proton therapy shows promise in ameliorating secondary cancer induced by radiotherapy, including enhanced quality of life after treatment[2,3], improved tolerance to chemoradiotherapy regimens[4–6] and decreased incidence of radiation-induced complications such as leukopenia, a condition characterized by a low white blood cell count[7].

[1]Department of Radiation Oncology, Stanford University School of Medicine, Stanford, CA, USA. [2]Center for Proton Therapy, Paul Scherrer Institute, Villigen, Switzerland. [3]Department of Radiation Oncology, Massachusetts General Hospital and Harvard Medical School, Boston, MA, USA. [4]SLAC National Accelerator Laboratory, Stanford University, Menlo Park, CA, USA. [5]Department of Medical Physics, Ludwig-Maximilians-Universität München (LMU Munich), Garching, Germany. [6]Department of Radiation Oncology, University of Washington, Seattle, WA, USA. [7]Division of Radiation Oncology, Fred Hutchinson Cancer Center, Seattle, WA, USA. [8]Biophysics Department, GSI Helmholtzzentrum für Schwerionenforschung, Darmstadt, Germany. [9]Institute for Condensed Matter Physics, Technische Universität Darmstadt, Darmstadt, Germany. [10]Department of Physics "Ettore Pancini", University Federico II, Naples, Italy. ✉e-mail: maradia@stanford.edu

Table 1 | Radiotherapy options

Radiotherapy type	Description	Advantages	Disadvantages
X-ray therapy	Utilizes high-energy X-rays to target tumours.	Widely accessible and effective for treating various cancer types, with advanced imaging capabilities.	Can damage surrounding healthy tissue and may lead to substantial acute and late side effects.
Proton therapy	Employs protons to deliver targeted radiation doses with minimal dose delivered to tissues beyond the tumour.	Reduces radiation exposure to healthy tissues and has a lower risk of secondary cancers.	Higher cost, limited availability as it requires specialized facilities.
Helium-ion therapy	Utilizes helium ions, offering better dose localization than protons with reduced lateral scattering.	Provides better tumour control while sparing normal tissue.	Limited availability as it requires specialized facilities, more costly than proton therapy.
Carbon-ion therapy	Uses carbon ions for a more targeted approach than with protons and helium.	Higher biological effectiveness in radio-resistant tumours compared with healthy tissue.	Expensive and less widely available, needs longer treatment planning time.
Brachytherapy	Involves placing radioactive sources directly inside or near the tumour.	Allows for high doses of radiation while sparing surrounding tissue.	Requires highly precise placement, often invasive, and not suitable for all tumour types.

A proton therapy system consists of three main components: an accelerator, a beam transport system and a gantry. The accelerator, which can be a cyclotron, synchrotron or synchrocyclotron, generates high-energy protons required for treatment. Once accelerated, these protons travel through a fixed beamline in the beam transport system, which directs and shapes the beam as it moves from the accelerator to the treatment room. The final component, the gantry, is a rotating structure that allows for precise beam delivery from multiple angles. By rotating around a horizontal axis, the gantry enables clinicians to target the tumour from various directions, ensuring optimal dose distribution while minimizing exposure to surrounding healthy tissues. Figure 2 illustrates a typical cyclotron- or synchrocyclotron-based proton therapy facility.

Since its modest origins, proton therapy has evolved through successive innovations in accelerator design, engineering and application. This Review focuses on these technological advancements and discusses potential future directions for the continued evolution of proton therapy's accelerator technology.

Accelerators for proton therapy

The first step in producing a proton beam is a source of protons that can be accelerated to treatment-level energies. Hydrogen is the most common proton source, with its electron removed using an electric field[8]. Once generated, the protons are accelerated to ensure that they have sufficient energy to reach the tumour's distal edge, which is the farthest point within the tumour. Cyclotrons and synchrotrons are commonly used for proton acceleration, but there is growing interest in developing linear accelerators (linacs) for this purpose.

Cyclotrons and synchrocyclotrons

Cyclotrons, invented in the 1930s, became the cornerstone of early proton therapy efforts and have been used for this purpose since the 1950s. The cyclotron accelerates charged particles, such as protons, in a circular path using alternating electric fields and a static magnetic field. Particles are injected and accelerated between D-shaped electrodes, while a magnetic field causes them to spiral outward. Synchronized electric fields boost their energy with each revolution. Once particles reach the desired energy level, they are extracted for applications, such as proton therapy or nuclear physics research[9].

Modern cyclotrons for proton therapy have fixed energies of 230 or 250 MeV and are compact[10,11]. To shrink a cyclotron's diameter, stronger magnetic fields are needed, which is achievable through superconducting coils. However, in cyclotrons with very strong magnetic fields (4–10 T), iron saturation prevents the iron core from increasing magnetic flux beyond a certain point, and along with coil geometry this causes the field strength to decrease with radius, limiting particle containment at larger radii[9]. This elongates the time for one revolution, reducing the particles' energy and eventually leading to their loss. To counteract this, the frequency of the radiofrequency signal is lowered over time, matching the particles' revolution time. This process, known as frequency shifting, allows a group of particles to be accelerated from source to extraction while ensuring that others are not accelerated prematurely.

Synchrocyclotrons were originally developed in 1945 to address the relativistic limitations of standard cyclotrons by modulating the radiofrequency to keep particles in sync as their mass increases at higher energies. Unlike conventional cyclotrons, which produce a continuous beam, synchrocyclotrons generate a pulsed beam, but can achieve higher energies without requiring substantially larger magnetic fields. Modern superconducting synchrocyclotrons have been adapted for proton therapy due to their compact size, reduced energy losses and lower shielding requirements, making them a cost-effective alternative to conventional cyclotrons.

For effective tumour treatment, varying beam energies—ranging from 70 to 230 MeV—are required to distribute the dose across the tumour's depth. In (synchro)cyclotron-based facilities, beam energy is reduced using energy degraders, but scattering in these materials (for example carbon or boron carbide) increases beam emittance and momentum spread, necessitating the use of collimators and slits in an energy selection system to minimize losses in the beamline[12]. Currently, most cyclotron-based facilities maintain a maximum emittance, which indicates how spread out a particle beam is in terms of both its position and angle, of 30π mm mrad, limiting transmission of low-energy beams with energies between 70 MeV and 100 MeV to around 0.1% from the cyclotron to the patient[13].

By using other degrader materials, such as boron carbide[14] and beryllium[15], the transmission can be improved by up to 50% for low-energy beams. Additionally, employing asymmetric collimators, optimizing the energy selection system and using specifically designed gantry beam optics can enhance transmission by around a factor of five[12,16,17]. Combining these methods could lead to almost a 100-fold increase in transmission compared with current facilities[18].

To achieve precise and efficient treatment delivery, cyclotrons offer numerous benefits, such as a continuous beam, adjustable beam intensity, rapid and precise intensity control, high reliability due to minimal components, and a relatively small spatial footprint. However, there are drawbacks to consider: cyclotrons can become radioactive due to beam losses; they offer only a fixed energy, requiring a degrader in the beamline for energy adjustment, and components near the degrader can become activated as well.

https://doi.org/10.1038/s41567-025-02994-7

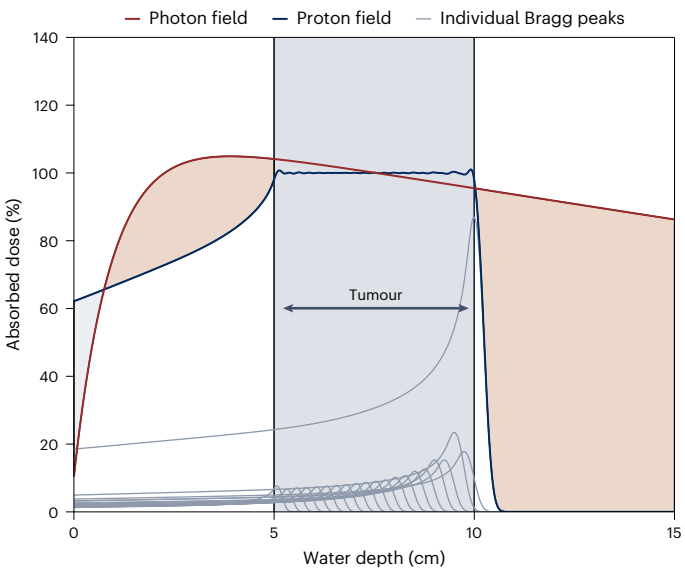

Fig. 1 | Absorbed dose as a function of water depth for photons and protons. A dosimetric comparison of conventional radiotherapy with 10-MV photons (red) and proton therapy (blue). The spread-out Bragg peak is a superposition of individual Bragg peaks (grey). The grey-shaded area represents the tumour's size, the blue-shaded area primarily corresponds to the skin and the red-shaded area indicates healthy brain tissue. Figure reproduced with permission from ref. 53, V. Maradia.

FLASH proton therapy is an innovative technique that delivers ultrahigh dose rates of radiation (>40 Gy s^{-1}) in a fraction of a second, demonstrating promising results in preserving normal tissues while effectively targeting tumours. Currently, (synchro)cyclotrons are used at high energies (250/230 MeV) to achieve these FLASH dose rates[19]. The improved transmission capabilities of (synchro)cyclotron beamlines may help achieve FLASH dose rates across all energy beams while maintaining the Bragg peak for optimal treatment precision.

Although current cyclotrons focus on proton acceleration, there are ongoing developments for heavier-particle acceleration, such as helium or carbon ions.

Synchrotrons

Synchrotrons were proposed in the mid-1940s, and used for proton therapy in 1969[20]. A synchrotron consists of an injector, a ring of magnets, a beam pipe that is guided through the magnets, an accelerating structure and a beam extraction mechanism. By passing the beam repeatedly through the accelerating structure and synchronizing the ramp of the magnetic field with increasing particle momentum to maintain a constant orbit, charged particles can be accelerated. This method allows for complete electromagnetic control of the beam energy by stopping the acceleration at preprogrammed energies up to and including the maximum energy of the synchrotron.

Synchrotrons do not require a mechanical degrader to reduce the beam energy. Moreover, a synchrotron contains multiple small magnets rather than one large magnet as required for a cyclotron, which simplifies installation, maintenance and upgrades. Other advantages of synchrotrons are that—due to minimum beam losses—radiation levels are not as high as for cyclotrons and that fewer or lighter components are needed in the beamline[21]. Synchrotron rings are, however, larger in diameter than their cyclotron counterparts (5–20 m compared with 1.5–4.3 m; refs. 21–23), although other factors contribute to the overall facility size, such as the injector in the former or additional shielding requirements in the latter.

The main drawback of synchrotrons is the pulsed nature of the beam, meaning that the beam is turned off for the acceleration and injection parts of the treatment delivery. This negatively impacts the irradiation time. Considerable effort has been made to reduce the irradiation time and footprint of synchrotrons. The number of protons per extraction process has been improved through multiturn injection and raising the injection energy. Higher-energy injection provides more captured beam per pulse[23] through improved matching of the beam phase space to the synchrotron acceptance, through reduction in defocusing due to space-charge forces, which occur when particles repel each other due to their like charges, and by raising ring magnetic fields substantially above the residual fields of the ring magnets[24–26], but at increased cost and size of the injector.

In addition, the rise of pencil beam scanning, where a narrow, focused beam of protons is scanned across the tumour in a grid-like pattern, over the past decade has helped to reduce the irradiation time, as it uses almost 100% of the protons in the synchrotron beamline to treat patients. There is, however, renewed interest in increasing the average dose rate even further for FLASH and to mitigate the interplay effect, as we will discuss later. In addition to the high average dose rate, FLASH treatment requires at least 4 Gy per treatment session or fraction, roughly double that of a typical treatment. Achieving both requirements in a synchrotron with a small footprint is challenging due to space-charge limitations in the ring[25,27].

Similarly, narrow, precisely targeted beams of protons delivered in a grid-like pattern, so-called minibeams, allow for high doses of radiation to be concentrated on tumours while sparing surrounding healthy tissue. These beams may also be combined with the FLASH effect[28] to achieve FLASH with synchrotrons as minibeams do not overlap laterally in the entrance region, hence high dose and dose rates could be delivered for each beam sequentially.

Linear accelerators

Linacs are ubiquitous in the medical accelerator technology sector as the source of few-megaelectronvolt electrons to produce X-rays for conventional radiation therapy. However, linac technology has not been readily commercialized to produce therapeutic proton beams. Unlike electron beams, which attain relativistic speed at a beam energy of only a couple of megaelectronvolts, proton beams stay far below relativistic speeds even up to the highest beam energy needed for therapeutic applications, typically around 230 MeV. The design of a linac structure for a relativistic beam can rely on a reasonable approximation that the beam is simply travelling at the speed of light and can therefore use a uniformly periodic cavity design regardless of beam energy. At non-relativistic beam energies, the structure must accommodate the changing travel time of the beam through each section of the accelerator as the beam gains energy, introducing complexity and inhomogeneity to the design. Furthermore, the comparatively high beam energy requires an accelerator much longer than conventional medical electron linacs.

Accelerator technology for proton beams has been thoroughly explored and developed for high-energy physics applications, with CERN's Large Hadron Collider as today's most recognized example. The maturity of this technology has opened the door to applying these designs to proton therapy[29,30]. Instead of relying on an energy range shifter in the proton beam path, which limits the speed of changes and can increase in emittance of the beam, rapid adjustments to the amplitude and phase of the radiofrequency energy used to drive a linac can enable high-speed control of the final proton energy. Research conducted at SLAC National Accelerator Laboratory has investigated the development of a normal-conducting standing wave linac in which each accelerating cell receives radiofrequency power from its own compact klystron. This enables maximum flexibility in the phase and amplitude driving the acceleration, meaning that the linac can operate efficiently over a broad range of desired proton energies[31]. SLAC will test this radiofrequency-driven proton beam scanning system to enable high-dose-rate treatment modalities, such as FLASH therapy[32].

https://doi.org/10.1038/s41567-025-02994-7

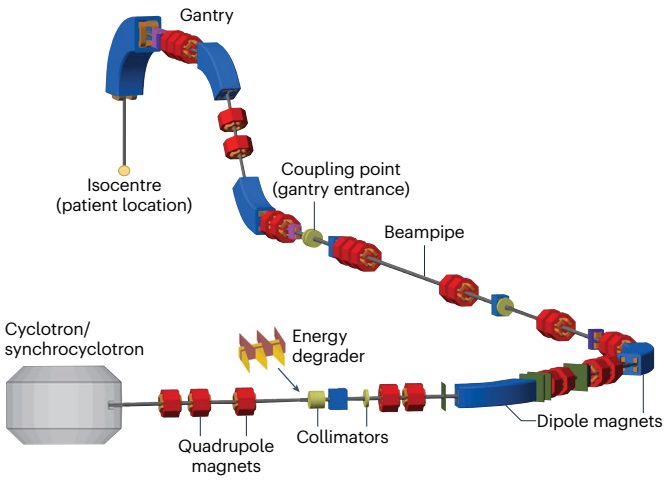

Fig. 2 | Schematic layout of a cyclotron- or synchrocyclotron-based proton therapy system. The machine consists of three main components: (1) an accelerator (cyclotron or synchrocyclotron) that generates a 250-MeV or 230-MeV proton beam, (2) a fixed beamline that transports the beam from the accelerator to the gantry entrance, incorporating an energy degrader, quadrupole magnets, dipole magnets and collimators for beam shaping, and (3) a rotating gantry that directs the beam to the patient, enabling dose delivery from multiple angles. Figure adapted with permission from ref. 53, V. Maradia.

Accelerators for heavy-ion therapy

Radiotherapy with charged particles heavier than protons is attractive, for both physical and biological reasons[33]. Heavy ions have a reduced lateral scattering compared with protons (Fig. 3a), which makes the dose gradients much sharper[34]. A measure for the energy deposited by charged particles as they travel through a medium is the linear energy transfer, where higher values indicate greater biological effectiveness and higher potential for damaging cancer cells. Compared with sparsely ionizing photons and protons with low linear energy transfer[35], heavy ions with high linear energy transfer are much more efficient in destroying cancer cells. The increased relative biological effectiveness of heavy ions compared with protons can, however, lead to a higher risk of toxicity on normal tissue. The relative biological effectiveness for cell killing increases with linear energy transfer and depends on the dose, dose rate and inherent susceptibility of different cell types to damage from radiation or harmful agents, influenced by factors such as genetics, cell cycle phase and DNA repair capability.

The ideal particle for radiotherapy would have a low linear energy transfer in the entrance channel, where the normal tissue is exposed, and a high linear energy transfer in the spread-out Bragg peak, at the tumour location. Carbon represents a good compromise, which is why ^{12}C ions were chosen for use in cancer therapy[36,37]. Currently, 118 proton therapy centres are in operation, having treated over 320,000 patients with protons by the end of 2023, whereas 14 carbon-ion centres are in operation, with more than 57,000 patients treated with carbon ions by the same time[38,39], and many more centres under construction.

In current systems, the linear energy transfer of carbon ions is quite diluted along the spread-out Bragg peak, especially for large tumour volumes[40]. Therefore, carbon-ion therapy does not fully exploit the radiobiological properties of radiation with high linear energy transfer[41]. It is possible to increase the linear energy transfer in the gross tumour volume with different beam delivery strategies or using heavier ions such as oxygen[42]. Ideally, multi-ion treatments would allow high linear energy transfer in the target and low linear energy transfer in normal tissue[43].

Another interesting ion for therapy is helium[44], which has a lateral spread that is similar to that of carbon, and thus better than protons (Fig. 3a). From the radiobiological point of view, the linear energy transfer is—similarly to that of protons—low, which makes helium safe also for paediatric patients. Over 2,000 patients were treated with helium ions during a heavy-ion pilot project between 1975 and 1992 (ref. 45). Almost 30 years after the shutdown of this pilot project, one patient was treated again with helium ions at the Heidelberg Ion Therapy centre in Germany, where helium ion therapy is now planned for routine use along with protons and carbon ions[46].

The main accelerator challenge in heavy-ion therapy compared with protons is that it relies on larger and more expensive machines. The most bulky technological components are the accelerator itself and the gantry. The size of these machines increases with the particle kinetic energy per nucleon and the mass-over-charge ratio. Accelerators are designed to reach a desired range in water-equivalent tissue, which refers to any material that interacts with radiation similarly to water, because human tissues consist mostly of water. This range is typically 30 cm, which corresponds to a particle-specific kinetic energy, such as 430 MeV per nucleon for carbon or 220 MeV for protons. As shown in Fig. 3c, the corresponding magnetic rigidity, a measure of a charged particle's resistance to bending in a magnetic field, increases substantially with ion mass. Therefore, heavy-ion accelerators will have a larger spatial footprint, resulting in a substantial increase in cost.

Currently all accelerators for heavy ions are synchrotrons. However, a carbon-ion clinical cyclotron is currently under commissioning in Caen (France)[47]. In either case, the research effort to democratize heavy-ion therapy is focusing on reducing the magnetic rigidity to achieve smaller spatial footprints[48]. These efforts are mostly directed toward the use of superconducting magnets[49], which increase the strength of the magnetic field (from around 1.8 T in resistive magnets to 4–9 T for superconductive), thus allowing a reduction of the radius at the same rigidity. In Japan[50], work towards a multi-ion synchrotron (hydrogen, helium, carbon and oxygen ions with energies up to 430 MeV n^{-1}) is ongoing. By using niobium–titanium superconducting wires and optimized beam optics, the device is expected to have half the circumference of current heavy-ion medical accelerators. However, there are several hurdles to building magnets with high fields, high ramp rates and fast cycling, required to change energy in small steps, using current superconductive technology. High-temperature superconductors may provide a breakthrough in this direction[51], but they are still in experimental testing. Further research and development in superconductive magnets is likely to lead to substantially smaller and cheaper[52,53] heavy-ion machines in the next ten years.

Innovations in proton and ion beam therapy delivery techniques

There are two main lines of innovation in treatment delivery approaches that may substantially change the proton and ion beam therapy landscape in the next decade: treatment geometries as well as ultrahigh dose rates and the FLASH effect.

New treatment geometries

Nearly all radiation oncology treatments are delivered by rotating the beam around a patient lying in a prone or supine position. In proton therapy, this requires the construction of gantries that—due to the magnetic rigidity of protons—are large (around 10 m in diameter), heavy (around 100 ton) and expensive. In addition, there is the engineering challenge of maintaining a 1-mm rotational accuracy over 15–20 yr of continuous use. In the past decade, there have been efforts to produce smaller and cheaper systems by reducing the available beam angles[54] or by redesigning the energy selection and beam delivery system, so that the accelerator is mounted on a rotating gantry[55]. There is now increasing interest in making an additional step towards size reduction, designing treatment solutions with a fixed horizontal line with the patient either sitting or standing on a rotating positioning system[56]. In addition to the further reduction in the spatial footprint, complexity

https://doi.org/10.1038/s41567-025-02994-7

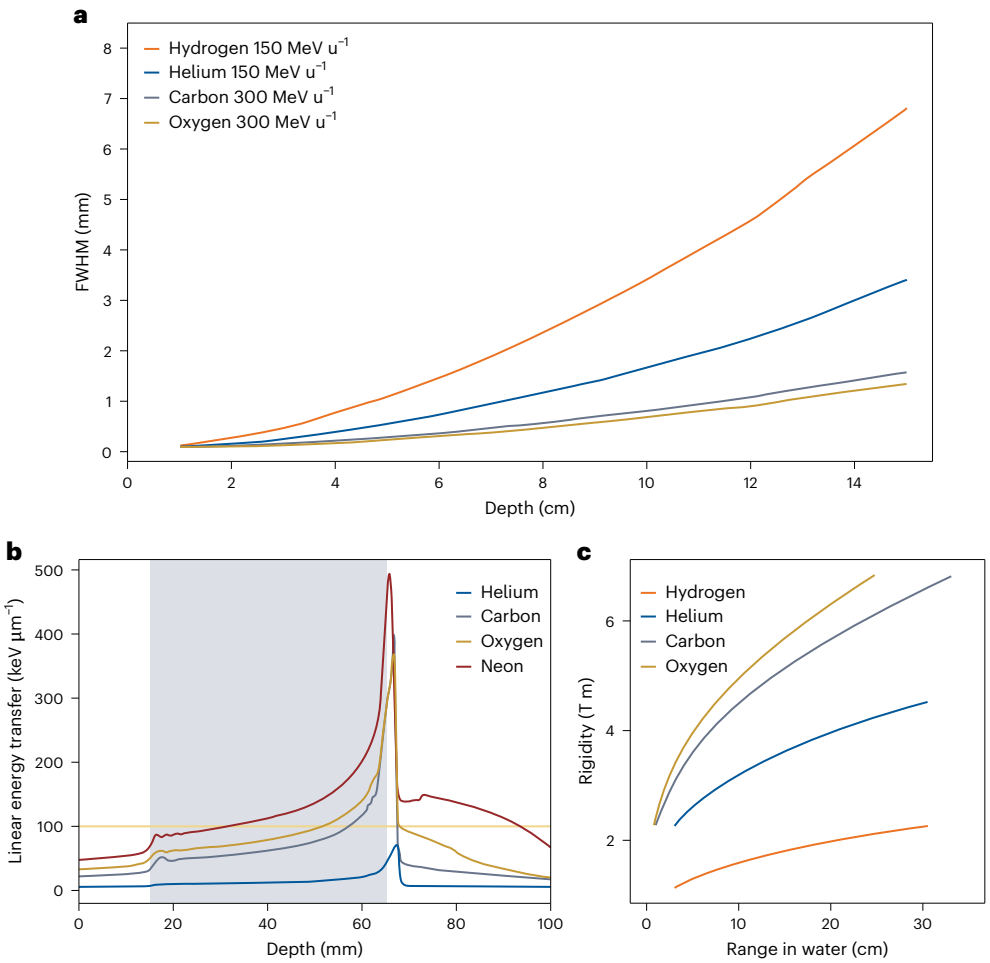

Fig. 3 | Physical properties of heavy-ion beams for therapy. a, Lateral spread of different ions in water, obtained from Monte Carlo simulations. The *y* axis shows the full-width at half-maximum (FWHM) of the Gaussian fit of the beam spot distribution for hydrogen, helium, carbon and oxygen ions reaching a depth of 15 cm in water. **b**, Linear energy transfer versus depth in tissue for a single spread-out Bragg peak for helium, carbon, oxygen and neon ions providing a uniform physical dose (2 Gy). The grey area represents the tumour region, a $2.5 \times 2.5 \times 5$ cm^3 volume centred at 4 cm in water. The yellow line represents the 100-keV-µm^{-1} level. **c**, Magnetic rigidity of hydrogen, helium, carbon and oxygen ions as a function of their range in water. Panel **a** reproduced with permission from ref. 34, IOP.

and cost, this will facilitate high-quality imaging, such as dual-energy computed tomography (discussed below) in treatment position, and may increase the number of patients receiving heavier-ion treatments, where rotating gantries are typically unavailable.

However, the transition to this new treatment geometry faces several technical issues. Diagnostic images that are routinely used for treatment planning, such as magnetic resonance imaging or positron emission tomography, are acquired in supine position, which is not going to change for the foreseeable future. In principle, the problem can be tackled with dedicated deformable image registration methods that align images of the same anatomical area taken at different times or with different modalities by allowing complex shape changes, but a substantial difference between imaging position and treatment position will inevitably result in an additional source of uncertainty. The extensive knowledge accumulated in radiation oncology about intrafraction motion, referring to the movement of a tumour or surrounding tissues during a radiation therapy session due to breathing, for example, is based on patients lying down, and it remains to be seen how much of it can be translated to a sitting or standing position. Not all beam configurations currently being used may be achievable. This question has been addressed in a planning study including seven head-and-neck and brain tumours[57], but additional systematic analysis is necessary.

The clinical experience of the centres that will soon implement upright proton therapy for a broad spectrum of clinical indications will be crucial to achieve a full assessment of the trade-offs associated with this approach. Nevertheless, there may be situations, such as in the treatment of frail patients or paediatric patients under anaesthesia, where the conventional geometry remains the best option.

Ultrahigh dose rate and FLASH

Although an increased radiation resistance of healthy tissues at ultrahigh dose rates exceeding 40 Gy s^{-1} was observed decades ago[58], this phenomenon has recently come back to prominence and is now referred to as the FLASH effect[59]. Early FLASH treatment of a human patient was delivered with electrons[60], but proton therapy is the only approach allowing ultrahigh-dose-rate treatments for a broad spectrum of clinical indications with technology available in clinical environments. The clinical impact of FLASH over the next five to ten years will therefore be largely determined by the results achieved with ultrahigh-dose-rate proton therapy. Despite the capability of current proton therapy systems to reach such dose rates, these devices were designed for much lower dose rates[27]. Therefore, ultrahigh-dose-rate proton therapy requires redesign of treatment planning and delivery[61]. The two key bottlenecks of current systems in this regard are a rapidly decreasing beam transmission efficiency as a function of energy (generally <1% for energies

https://doi.org/10.1038/s41567-025-02994-7

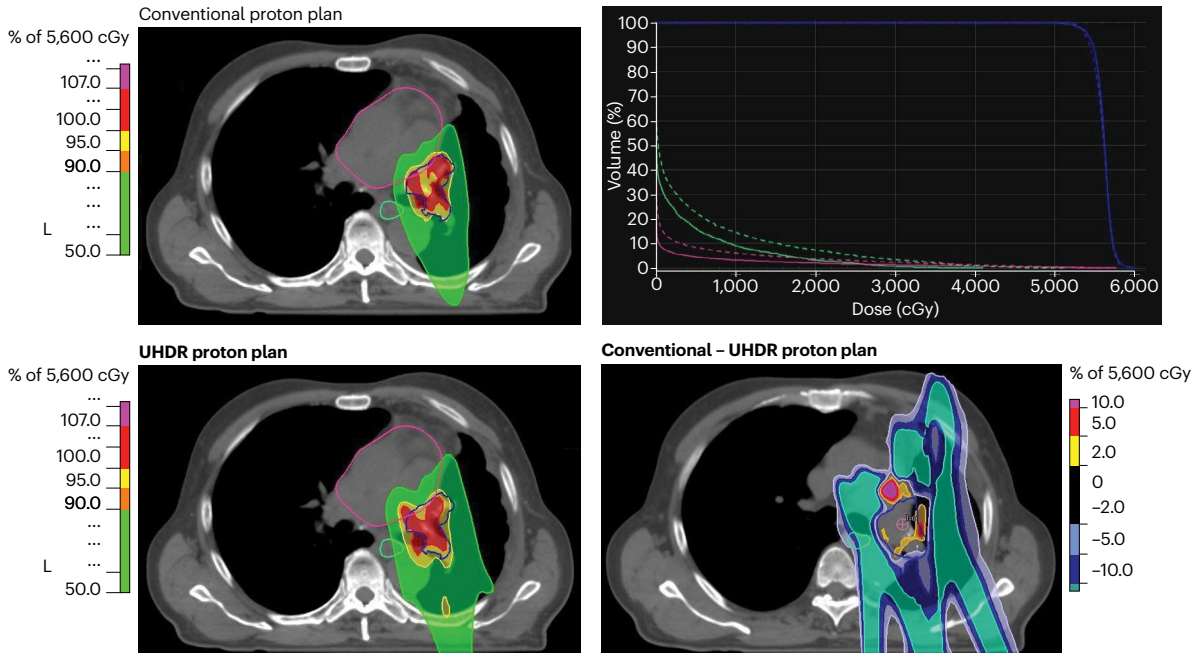

Fig. 4 | Comparison between a conventional and an ultrahigh-dose-rate proton therapy plan. In the latter case, a range shifter, a three-dimensional range modulator and an aperture were combined to enable the treatment delivery. Left: the target volume is show as a blue contour. The large pink contour represents the heart, whereas the green contour outlines the oesophagus. In the colour wash distribution, green, yellow and red show 50%, 95% and 100% of the prescribed dose, respectively. In the high-dose region (95% and 100% of the prescribed dose region) the two dose distributions are very similar, whereas at lower dose levels (50% or less of the prescribed dose region) the ultrahigh-dose-rate plan is slightly inferior. Upper right: the cumulative dose–volume histogram, with the blue line representing the dose to the target, the pink line that to the heart and the green line that to the oesophagus. Solid lines indicate the dose distribution from the conventional proton plan, whereas dashed lines represent the ultrahigh-dose-rate (UHDR) proton plan. Lower right: the difference between the two distributions normalized to the prescribed tumour dose. Both plans comply with the clinical requirements set for this patient.

below 100 MeV) and the time required for changing the proton energy (depending on the machine, each energy change takes between 80 ms and 2,000 ms; ref. 62). This means that current ultrahigh-dose-rate proton treatments are delivered with a single predefined energy, namely the highest available, which can be achieved with two methods. In a 'shoot-through' approach[63], the distal end of the Bragg peak is located outside the patient. This approach has the advantage of not requiring beam-specific hardware; it has been tested in multiple planning studies and has been used in a proton trial on human patients[64]. The other approach combines a range shifter, which adjusts the proton beam's penetration depth to target tumours more accurately, a three-dimensional range modulator for fine-tuning the range of protons for precise dose distribution[65,66] and an aperture that shapes the dose distribution laterally to conform to the tumour's contours to achieve dose conformality. This approach has the disadvantage of requiring patient- and field-specific equipment tailored for individual patient treatments in proton therapy, designed to optimize dose delivery on the basis of the unique characteristics of each tumour and its surrounding tissues, but it allows dose distributions that are much closer to those of a conventional proton therapy plan to be achieved (see Fig. 4).

There are still radiobiology research questions on which beam delivery parameters are key to benefit from FLASH[67]—for example, what the minimum dose rate or minimum dose per fraction is, or the effect of fractionation[68] and of 1–2-min-long pauses within a fraction[69,70]. Therefore, current research efforts in ultrahigh-dose-rate proton therapy aim for the development of new beam delivery approaches that address the limitations of existing systems, the maximization of the dose rate achievable by explicitly including dose rate metrics in the optimization cost function[71] or optimizing the spot delivery sequence[72] and the investigation of ultrahigh dose rates for applications other than FLASH—for example, to address the issue of breathing or cardiac motion[73] during treatments.

Imaging in particle therapy

Full clinical exploitation of the aforementioned physical and biological advantages of particle beams for radiotherapy is still hampered by uncertainties in the delivery of the intended treatment. A major obstacle to overcome in clinical practice is the uncertainty in the knowledge of the stopping position of ions in the patient due to the limited understanding of the tissue-stopping properties with respect to water in which the clinical beams are calibrated[74]. Another issue pertains to changes of the treatment with respect to the planning situation—for example, anatomical variations and organ motion, caused by gastrointestinal, cardiac and respiratory motion[75]. To this end, several efforts are ongoing to directly integrate imaging in the treatment site, ideally with the patient already in position and even during treatment.

X-ray and ion imaging

For improved accuracy in the knowledge of the stopping power properties of the patient tissue relative to water, the so-called stopping power ratio, one issue to resolve is the ambiguous calibration of the typically used single-energy-spectrum X-ray computed tomography, which often lacks specificity in differentiating between various tissue types and their corresponding attenuation characteristics. To overcome this limitation, different variants of advanced multienergy X-ray imaging are being put forward. Several studies have shown the superiority of computed tomography using two different X-ray energy spectra (dual energy) at the source or detector level to better differentiate between tissue types and photon counting to provide highly detailed imaging for retrieval of the stopping power ratio in tissue-equivalent phantoms, ex vivo samples and even human applications[76,77]. This is due to their ability to better disentangle the relevant physical dependences of the stopping power ratio on the tissue effective atomic number and relative electron density. Although the adoption of advanced X-ray diagnostics in particle therapy is still relatively slow, ongoing efforts

https://doi.org/10.1038/s41567-025-02994-7

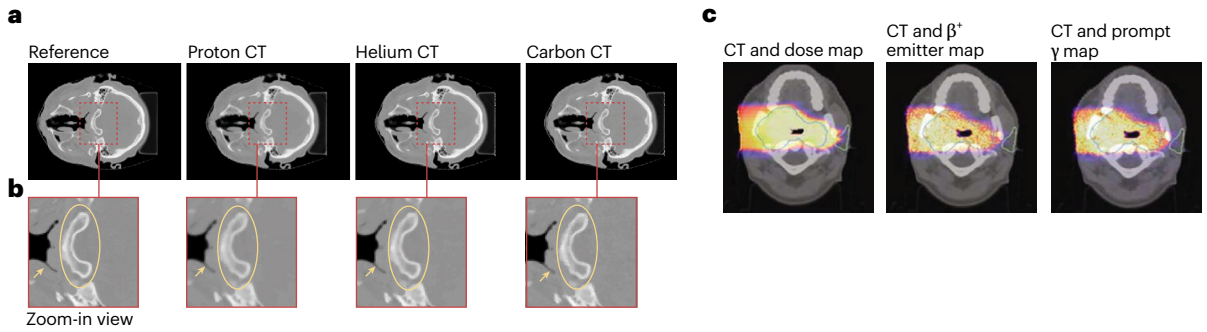

Fig. 5 | Examples of advanced imaging techniques in particle therapy. **a**, Comparison of axial slices of a reference X-ray computed tomography image calibrated using stopping power ratio (left) with the reconstructed ion computed tomography (CT) images simulated for proton and helium- and carbon-ion beams delivering the same physical dose and imaged with an ideal single-particle tracking detector[83]. **b**, Enlarged views of a selected region within the images of **a**, with arrows and ellipses indicating anatomical features imaged with different levels of spatial resolution and contrast in the considered scenarios. **c**, Different modalities for treatment verification of the planned dose (left). The simulated spatial distributions of irradiation-induced positron emitters (middle) and prompt gamma yields (right) are well correlated to the planned dose. All distributions (the contour represents the target volume and coloured maps show the comparison of dose, with red showing high intensity and blue showing low intensity) are superimposed onto the same representation of the patient given in greyscale by an X-ray computed tomograph. Panel **c** adapted from Figure 5 in ref. 108 under a Creative Commons license CC BY 4.0, G. Dedes.

aim to develop customized solutions for computed tomography integrated into treatment sites that make use of fan-shaped X-ray beams for high-resolution two-dimensional imaging on a helical trajectory or of cone-shaped X-ray beams for capturing larger volumes of data in three dimensions[78,79]. These solutions will offer multienergy acquisition capabilities in three and even four dimensions, enhancing dosimetric calculations in online adaptive radiotherapy workflows.

Because X-ray imaging methods still rely on calibration procedures with tissue-equivalent materials and entail a non-negligible radiation burden, especially in the envisioned prospect of daily adaptation, a promising alternative is to directly determine the stopping power ratio by imaging the patient using the same type of radiation as employed for treatment. In first approximation, the stopping power ratio is independent of energy and of ion type. Therefore, it can be determined at sufficiently high energies where the ions traverse the patient and then be applied to estimate the ion stopping position in the tumour at the clinically used lower therapeutic energies. For this purpose, several detector concepts, in particular from high-energy physics, are being explored[80]. The most advanced solutions aim at tracking the position and direction of individual particles before and after the patient and then determine their exit residual energy by complete stopping in a range telescope or calorimeter[81] or by a time-of-flight measurement in the same detectors as used for particle tracking[82]. Due to the practical limits of what data rates can be processed for single-particle detection, accelerator and beam delivery systems must reduce the beam intensity relative to therapeutic levels while maintaining the capability to monitor and steer the beam. The latter is particularly important for ion imaging using pencil beam scanning. Achieving this requires a wide dynamic range of beam currents, especially in machines designed for ultrahigh-dose-rate delivery, such as those intended for exploiting the FLASH effect[28].

In selecting the ideal ion species for imaging, it is essential to consider trade-offs, particularly regarding spatial resolution, stopping power retrieval accuracy and imaging. These aspects are driven by lateral scattering that reduces spatial resolution for lighter ions, range straggling that increases stopping power retrieval accuracy for heavier ions and linear energy transfer or nuclear fragmentation reactions that increase imaging dose for heavier ions (Fig. 3a,b)[83]. In this regard, helium has been suggested to offer an optimal compromise. However, the increasing ion charge constrains the achievable highest beam energies, whereas compact proton synchrotrons produce beams with energies up to 330 MeV to support transmission imaging applications in addition to therapy. Another intriguing idea is to exploit the possibility to accelerate different ion species with equal charge-over-mass ratio, such as ^{4}He and ^{12}C, in the same machine. Given the different penetration depths at the attained kinetic energies up to around 450 MeV u^{-1}, this opens up the prospects of stopping the less penetrating ^{12}C ions in the tumour, while using the longer-ranging ^{4}He for simultaneous radiographic imaging[84]. Having various ion species available at the same treatment site will allow for the selection of the most suitable ion species for the imaging required for planning the treatment (Fig. 3a,b), regardless of which ion species is utilized for dose delivery.

Although advanced X-ray and ion imaging solutions could be used to track patient motion and its consequence for range variations with respect to the initial treatment plan, ideally informing a real-time correction, soft-tissue contrast of these techniques remains poor. Therefore, correct identification of the tumour and organs at risk for a reliable adaptation is challenging. Hence, another promising development is the integration of magnetic resonance image guidance in particle therapy, requiring us to overcome the unfavourable interference of the electromagnetic fields on beam delivery and imaging. To this end, human-scale magnets with a field strength between 0.2 and 0.5 T are being integrated in experimental beamlines of pencilbeam scanning delivery, along with the exploration of technologically less complex solutions relying on low magnetic fields of less than 0.1 T (ref. 85).

Positron emission tomography and prompt gamma-ray imaging

Whereas the techniques described so far focus on capturing the correct description of the patient anatomy and its stopping properties shortly before or even during treatment, other imaging methods aim at detecting irradiation-induced physical emissions to infer information on the actual beam range and delivered dose during treatment (Fig. 5)[86]. In the context of conventional radiotherapy beams, recent progress in positron emission tomography has opened the prospect of quasi-real-time imaging, despite the limitations of the finite (from milliseconds to several minutes) half-life of the created isotopes, and the challenges of biological washout in the time elapsing between isotope creation and detection of annihilation photons[87,88]. The latter is the process by which radioactive isotopes are gradually removed or redistributed in the body, potentially compromising the accuracy of real-time imaging and dosage information in radiation therapy. In addition, positron emission tomography may enable direct imaging of the stopping position of radioactive ions to verify the correct dose delivery[89].

To overcome the intrinsic shortcomings of positron emission tomography, such as non-negligible half-life, positron range and

biological washout, for accurate, real-time monitoring of the treatment delivery, considerable research efforts are being directed to the more challenging detection of the energetic photons released in fast (subnanosecond) deexcitation nuclear processes. Prototypes of collimated cameras are reaching the stage of clinical evaluation for detection of these prompt gamma rays generated by individual proton pencil beams delivered to the patient, possibly also resolved in energy[90,91]. In addition to less mature concepts that explore combined detection of multiple nuclear emission products[92], including charged particles and neutrons[93], there are also techniques that are more intrinsically linked to the energy deposition mechanism rather than nuclear reaction processes. Especially with the development of accelerators delivering intense pulses on microsecond timescales, such as compact synchrocyclotrons or novel linac solutions, the detection of radiation-induced thermoacoustic emissions is receiving renewed attention. This could pave the way to a cost-effective solution providing quasi-real-time multilateration of the Bragg peak position and even two- or three-dimensional reconstruction of the delivered dose, co-registered to the underlying anatomical location for sites that can be accessed using ultrasound imaging[94]. This is especially of interest in combination with the latest developments of FLASH[95] and minibeam therapy, which are both expected to enhance the strength of the thermoacoustic emissions for easier detectability.

Outlook

Accelerators for particle therapy are continually being developed further. Future synchrotrons will probably have faster irradiation times and smaller spatial footprints. This may be accomplished through more compact injectors providing beams with higher energy or wider adoption of multiturn injection, where multiple pulses of particles are injected over several turns to increase beam intensity and density without requiring a larger injector. Reducing the spatial footprint of accelerators can be achieved with highly pulsed, normal-conducting magnets[96,97] that operate in short, powerful bursts instead of continuously. This approach allows for smaller, less massive magnets that still maintain strong magnetic fields as needed, making them more compact and cost-effective—ideal for facilities with limited space. The smallest cyclotrons use superconducting magnets, a development that has not yet transferred to proton therapy synchrotrons due to the need for fast magnetic field changes[98]. If these challenges can be overcome, proton therapy synchrotrons could be superconducting[99] or fixed-field alternating-gradient-style machines[100].

Fixed-field alternating gradient accelerators extract beams at variable energy, as in a synchrotron, have the high-current, fixed-magnetic-field and variable-radiofrequency characteristics of a synchrocyclotron and have the capability to change energy faster than a rapid cycling synchrotron. In addition, the fixed-field alternating gradient accelerator lattice has large geometric and momentum acceptance[101]. They come in different types on the basis of how they manage energy changes: scaling accelerators maintain stable particle trajectories during acceleration[101,102], non-scaling types allow this stability to vary for greater efficiency[100] and quasiscaling types mostly keep it steady with slight adaptability[103]. Variable energy extraction is achieved by turning off the radiofrequency at the desired energy[104] and these accelerators can operate at fast cycling rates, reaching thousands of cycles per second (kilohertz range). These features are still under development.

Larger uncertainties are associated with the development of alternative accelerator technologies, such as laser-driven particle accelerators[105]. Although having great potential, those accelerators are still far from clinical applications as standalone machines for radiotherapy[106]. However, using lasers as injectors in superconducting synchrotrons may result in a substantial reduction in spatial footprint and appears more realistic, given that the injection energy is of the order of 10 MeV. Plans in this direction are currently ongoing in Japan[50] and in the UK[107].

In addition to offering personalized and effective cancer treatment strategies, advancements in particle therapy could lead to reduced side effects and an enhanced quality of life for patients. As research continues, particle therapy may play an increasingly vital role in addressing complex cancer cases and improving overall patient outcomes.

References

1. Wilson, R. R. Radiological use of fast protons. *Radiology* **47**, 487–491 (1946).
2. Verma, V., Simone, C. B. & Mishra, M. V. Quality of life and patient-reported outcomes following proton radiation therapy: a systematic review. *J. Natl Cancer Inst.* **110**, 341–353 (2018).
3. Yock, T. I. et al. Quality of life outcomes in proton and photon treated pediatric brain tumor survivors. *Radiother. Oncol.* **113**, 89–94 (2014).
4. Baumann, B. C. et al. Comparative effectiveness of proton vs photon therapy as part of concurrent chemoradiotherapy for locally advanced cancer. *JAMA Oncol.* **6**, 237–246 (2020).
5. Chang, J. Y. et al. Phase 2 study of high-dose proton therapy with concurrent chemotherapy for unresectable stage III nonsmall cell lung cancer. *Cancer* **117**, 4707–4713 (2011).
6. Sejpal, S. et al. Early findings on toxicity of proton beam therapy with concurrent chemotherapy for nonsmall cell lung cancer. *Cancer* **117**, 3004–3013 (2011).
7. Shiraishi, Y. et al. Severe lymphopenia during neoadjuvant chemoradiation for esophageal cancer: a propensity matched analysis of the relative risk of proton versus photon-based radiation therapy. *Radiother. Oncol.* **128**, 154–160 (2018).
8. Brown, I. G. *The Physics and Technology of Ion Sources* (Wiley-VCH, 2004).
9. Schippers, M. in *Proton Therapy Physics* (ed. Paganetti, H.) 69–112 (CRC Press, 2018).
10. Kleeven, W. & Zaremba, S. Cyclotrons: magnetic design and beam dynamics. In *Proc. CAS-CERN Accelerator School on Accelerators for Medical Applications* Vol. 1 (ed. Bailey, R.) 177–239 (CERN, 2017).
11. van de Walle, J. et al. The S2C2: from source to extraction. In *CYC 2016—Proc. 21st International Conference on Cyclotrons and their Applications* (eds Chrin, J. et al.) 285–289 (JACoW Publishing, 2016).
12. Maradia, V. et al. A new emittance selection system to maximize beam transmission for low-energy beams in cyclotron-based proton therapy facilities with gantry. *Med. Phys.* **48**, 7613–7622 (2021).
13. Maradia, V. et al. Application of a scattering foil to increase beam transmission for cyclotron based proton therapy facilities. *Front. Phys.* **10**, 919787 (2022).
14. Gerbershagen, A. et al. Measurements and simulations of boron carbide as degrader material for proton therapy. *Phys. Med. Biol.* **61**, N337–N348 (2016).
15. Van Goethem, M. J., Van Der Meer, R., Reist, H. W. & Schippers, J. M. Geant4 simulations of proton beam transport through a carbon or beryllium degrader and following a beam line. *Phys. Med. Biol.* **54**, 5831–5846 (2009).
16. Maradia, V. et al. Increase of the transmission and emittance acceptance through a cyclotron-based proton therapy gantry. *Med. Phys.* **49**, 2183–2192 (2022).
17. Maradia, V. et al. A novel beam optics concept to maximize the transmission through cyclotron-based proton therapy gantries. In *Proc. IPAC2021* (eds Lin, L. et al.) 2477–2479 (JACoW Publishing, 2021); https://doi.org/10.18429/JACoW-IPAC2021-TUPAB407
18. Maradia, V. et al. Demonstration of momentum cooling to enhance the potential of cancer treatment with proton therapy. *Nat. Phys.* **19**, 1437–1444 (2023).
19. Favaudon, V. et al. Erratum for the Research Article: "Ultrahigh dose-rate FLASH irradiation increases the differential response between normal and tumor tissue in mice" by V. Favaudon, L. Caplier, V. Monceau, F. Pouzoulet, M. Sayarath, C. Fouillade, M.-F. Poupon, I. Brito, P. Hupé, J. Bourhis, J. Hall, J.-J. Fontaine, M.-C. Vozenin. *Sci. Transl. Med.* **11**, eaba4525 (2019).

20. Chuvilo, I. V. et al. ITEP synchrotron proton beam in radiotherapy. *Int. J. Radiat. Oncol. Biol. Phys.* **10**, 185–195 (1984).
21. Clasie, B. M., Letourneau, D., Schwarz, M., Seuntjens, J. & Maughan, R. L. Proton therapy equipment installation, upgrades, and building design. *Pract. Radiat. Oncol.* **14**, e249–e254 (2024).
22. Balakin, V. E. et al. Status of the proton therapy complex Prometheus. In *Proceedings of the 26th Russian Particle Accelerator Conference* (eds Kuzin, M. V. & Schaa, V. R. W.) 135–138 (JACoW Publishing, 2018); https://doi.org/10.18429/JACoW-RUPAC2018-FRXMH03
23. Coutrakon, G. B. Accelerators for heavy-charged-particle radiation therapy. *Technol. Cancer Res. Treat.* **6**, 49–54 (2007).
24. Johnsen, K. *Injection Philosophy for Synchrotrons* CERN-PS-KJ-30 (CERN, 1956).
25. Coutrakon, G. et al. A performance study of the Loma Linda proton medical accelerator. *Med. Phys.* **21**, 1691–1701 (1994).
26. Knaus, P. *Particle Stacking by Transverse Multi-Turn Injection in a Synchrotron for Medical Use*. Diploma thesis, Univ. Karlsruhe (1995).
27. Jolly, S., Owen, H., Schippers, M. & Welsch, C. Technical challenges for FLASH proton therapy. *Phys. Med.* **78**, 71–82 (2020).
28. Mazal, A. et al. FLASH and minibeams in radiation therapy: the effect of microstructures on time and space and their potential application to protontherapy. *Br. J. Radiol.* **93**, 20190807 (2020).
29. Amaldi, U. et al. LIBO—a linac-booster for protontherapy: construction and tests of a prototype. *Nucl. Instrum. Methods Phys. Res. A* **521**, 512–529 (2004).
30. Benedetti, S., Grudiev, A. & Latina, A. High gradient linac for proton therapy. *Phys. Rev. Accel. Beams* **20**, 040101 (2017).
31. Lu, X. et al. A proton beam energy modulator for rapid proton therapy. *Rev. Sci. Instrum.* **92**, 024705 (2021).
32. Schulte, R. et al. Transformative technology for FLASH radiation therapy. *Appl. Sci.* **13**, 5021 (2023).
33. Durante, M., Debus, J. & Loeffler, J. S. Physics and biomedical challenges of cancer therapy with accelerated heavy ions. *Nat. Rev. Phys.* **3**, 777–790 (2021).
34. Durante, M. & Paganetti, H. Nuclear physics in particle therapy: a review. *Rep. Prog. Phys.* **79**, 096702 (2016).
35. Tinganelli, W. & Durante, M. Carbon ion radiobiology. *Cancers* **12**, 3022 (2020).
36. Tsujii, H. et al. (eds.) *Carbon-Ion Radiotherapy: Principles, Practices, and Treatment Planning* (Springer, 2014).
37. Kraft, G. Tumor therapy with heavy charged particles. *Prog. Part. Nucl. Phys.* **45**, S473–S544 (2000).
38. *Patient Statistics* (Particle Therapy Co-Operative Group (PTCOG), accessed 23 July 2024); https://www.ptcog.ch/
39. Tommasino, F., Scifoni, E. & Durante, M. New ions for therapy. *Int. J. Part Ther.* **2**, 428–438 (2016).
40. Nachankar, A. et al. Planning strategy to optimize the dose-averaged LET distribution in large pelvic sarcomas/chordomas treated with carbon-ion radiotherapy. *Cancers* **15**, 4903 (2023).
41. Sokol, O. & Durante, M. Carbon ions for hypoxic tumors: are we making the most of them? *Cancers* **15**, 4494 (2023).
42. Sokol, O. et al. Oxygen beams for therapy: advanced biological treatment planning and experimental verification. *Phys. Med. Biol.* **62**, 7798–7813 (2017).
43. Ebner, D. K., Frank, S. J., Inaniwa, T., Yamada, S. & Shirai, T. The emerging potential of multi-ion radiotherapy. *Front. Oncol.* **11**, 624786 (2021).
44. Mairani, A. et al. Roadmap: helium ion therapy. *Phys. Med. Biol.* **67**, 15TR02 (2022).
45. Castro, J. R. Results of heavy ion radiotherapy. *Radiat. Environ. Biophys.* **34**, 48–48 (1995).
46. Tessonnier, T. et al. Commissioning of helium ion therapy and the first patient treatment with active beam delivery. *Int. J. Radiat. Oncol. Biol. Phys.* **116**, 935–948 (2023).
47. Chevalier, F., Lesueur, P. & Gaubert, G. CYCLHAD: a French facility dedicated for research and treatment in hadrontherapy. *Nucl. Phys. News* **32**, 27–31 (2022).
48. Graeff, C., Volz, L. & Durante, M. Emerging technologies for cancer therapy using accelerated particles. *Prog. Part. Nucl. Phys.* **131**, 104046 (2023).
49. Alonso, J. R. & Antaya, T. A. Superconductivity in medicine. *Rev. Accel. Sci. Technol.* **05**, 227–263 (2012).
50. Iwata, Y. et al. Design of a compact superconducting accelerator for advanced heavy-ion therapy. *Nucl. Instrum. Methods Phys. Res. A* **1053**, 168312 (2023).
51. Baird, Y. T. E. & Li, Q. Optimized magnetic design of superconducting magnets for heavy ion rotating gantries. *IEEE Trans. Appl. Supercond.* **30**, 4400108 (2020).
52. Yan, S., Ngoma, T., Ngwa, Wilfred & Bortfeld, T. Global democratisation of proton radiotherapy. *Lancet Oncol.* **24**, e245–e254 (2023).
53. Maradia, V. *Ultra-Fast Treatment Delivery to Enhance the Potential of Proton Therapy*. PhD thesis, ETH Zurich (2023).
54. Pidikiti, R. et al. Commissioning of the world's first compact pencil-beam scanning proton therapy system. *J. Appl Clin. Med. Phys.* **19**, 94–105 (2018).
55. Vilches-Freixas, G. et al. Beam commissioning of the first compact proton therapy system with spot scanning and dynamic field collimation. *Br. J. Radiol.* **93**, 20190598 (2020).
56. Volz, L., Sheng, Y., Durante, M. & Graeff, C. Considerations for upright particle therapy patient positioning and associated image guidance. *Front. Oncol.* **12**, 930850 (2022).
57. Yan, S. et al. Technical note: Does the greater power of pencil beam scanning reduce the need for a proton gantry? A study of head-and-neck and brain tumors. *Med. Phys.* **49**, 813–824 (2022).
58. Hornsey, S. & Bewley, D. K. Hypoxia in mouse intestine induced by electron irradiation at high dose-rates. *Int. J. Radiat. Biol.* **19**, 479–483 (1971).
59. Vozenin, M. C., Hendry, J. H. & Limoli, C. L. Biological benefits of ultra-high dose rate FLASH radiotherapy: Sleeping Beauty awoken. *Clin. Oncol.* **31**, 407–415 (2019).
60. Bourhis, J. et al. Treatment of a first patient with FLASH-radiotherapy. *Radiother. Oncol.* **139**, 18–22 (2019).
61. Schwarz, M., Traneus, E., Safai, S., Kolano, A. & van de Water, S. Treatment planning for Flash radiotherapy: general aspects and applications to proton beams. *Med. Phys.* **49**, 2861–2874 (2022).
62. Giovannelli, A. C. et al. Beam properties within the momentum acceptance of a clinical gantry beamline for proton therapy. *Med. Phys.* **49**, 1417–1431 (2022).
63. van de Water, S., Safai, S., Schippers, J. M., Weber, D. C. & Lomax, A. J. Towards FLASH proton therapy: the impact of treatment planning and machine characteristics on achievable dose rates. *Acta Oncol.* **58**, 1463–1469 (2019).
64. Mascia, A. E. et al. Proton FLASH radiotherapy for the treatment of symptomatic bone metastases: the FAST-01 nonrandomized trial. *JAMA Oncol.* **9**, 62–69 (2023).
65. Simeonov Y. et al. 3D range-modulator for scanned particle therapy: development, Monte Carlo simulations and experimental evaluation. *Phys. Med. Biol.* **62**, 7075–7096 (2017) (and corrigendum).
66. Maradia, V. et al. Universal and dynamic ridge filter for pencil beam scanning particle therapy: a novel concept for ultra-fast treatment delivery. *Phys. Med. Biol.* **67**, 225005 (2022).
67. Vozenin, M. C., Montay-Gruel, P., Limoli, C. & Germond, J. F. All irradiations that are ultrahigh dose rate may not be FLASH: the critical importance of beam parameter characterization and in vivo validation of the FLASH effect. *Radiat. Res.* **194**, 571–572 (2020).

68. Limoli, C. L. et al. The sparing effect of FLASH-RT on synaptic plasticity is maintained in mice with standard fractionation. *Radiother. Oncol.* **186**, 109767 (2023).
69. Mascia, A. et al. Impact of multiple beams on the FLASH effect in soft tissue and skin in mice. *Int. J. Radiat. Oncol. Biol. Phys.* **118**, 253–261 (2024).
70. Poulsen, P. R. et al. Oxygen enhancement ratio-weighted dose quantitatively describes acute skin toxicity variations in mice after pencil beam scanning proton FLASH irradiation with changing doses and time structures. *Int. J. Radiat. Oncol. Biol. Phys.* **120**, 276–286 (2024).
71. Ramesh, P., Gu, W., Ruan, D. & Sheng, K. Dose and dose rate objectives in Bragg peak and shoot-through beam orientation optimization for FLASH proton therapy. *Med. Phys.* **49**, 7826–7837 (2022).
72. José Santo, R., Habraken, S. J. M., Breedveld, S. & Hoogeman, M. S. Pencil-beam delivery pattern optimization increases dose rate for stereotactic FLASH proton therapy. *Int. J. Radiat. Oncol. Biol. Phys.* **115**, 759–767 (2023).
73. Maradia, V. et al. Ultra-fast pencil beam scanning proton therapy for locally advanced non-small-cell lung cancers: field delivery within a single breath-hold. *Radiother. Oncol.* **174**, 23–29 (2022).
74. Peters, N. et al. Experimental assessment of inter-centre variation in stopping-power and range prediction in particle therapy. *Radiother. Oncol.* **163**, 7–13 (2021).
75. Paganetti, H., Botas, P., Sharp, G. C. & Winey, B. Adaptive proton therapy. *Phys. Med. Biol.* **66**, 22TR01 (2021).
76. Wohlfahrt, P. et al. Clinical implementation of dual-energy CT for proton treatment planning on pseudo-monoenergetic CT scans. *Int. J. Radiat. Oncol. Biol. Phys.* **97**, 427–434 (2017).
77. Hu, G. et al. Assessment of quantitative information for radiation therapy at a first-generation clinical photon-counting computed tomography scanner. *Front. Oncol.* **12**, 970299 (2022).
78. Bogowicz, M. et al. Evaluation of a cone-beam computed tomography system calibrated for accurate radiotherapy dose calculation. *Phys. Imaging Radiat. Oncol.* **29**, 100566 (2024).
79. Peng, H. et al. Fan beam CT-guided online adaptive external radiotherapy of uterine cervical cancer: a dosimetric evaluation. *BMC Cancer* **23**, 588 (2023).
80. Johnson, R. P. Review of medical radiography and tomography with proton beams. *Rep. Prog. Phys.* **81**, 016701 (2018).
81. Schultze, B. et al. Particle-tracking proton computed tomography—data acquisition, preprocessing, and preconditioning. *IEEE Access* **9**, 25946–25958 (2021).
82. Krah, N., Dauvergne, D., Letang, J. M., Rit, S. & Testa, E. Relative stopping power resolution in time-of-flight proton CT. *Phys. Med. Biol.* **67**, 165004 (2022).
83. Meyer, S. et al. Dosimetric accuracy and radiobiological implications of ion computed tomography for proton therapy treatment planning. *Phys. Med. Biol.* **64**, 125008 (2019).
84. Volz, L. et al. Experimental exploration of a mixed helium/carbon beam for online treatment monitoring in carbon ion beam therapy. *Phys. Med. Biol.* **65**, 055002 (2020).
85. Pham, T. T. et al. Magnetic resonance imaging (MRI) guided proton therapy: a review of the clinical challenges, potential benefits and pathway to implementation. *Radiother. Oncol.* **170**, 37–47 (2022).
86. Parodi, K. Latest developments in in-vivo imaging for proton therapy. *Br. J. Radiol.* **93**, 20190787 (2020).
87. Ferrero, V. et al. Online proton therapy monitoring: clinical test of a silicon-photodetector-based in-beam PET. *Sci. Rep.* **8**, 4100 (2018).
88. Ozoemelam, I. et al. Feasibility of quasi-prompt PET-based range verification in proton therapy. *Phys. Med. Biol.* **65**, 245013 (2020).
89. Sokol, O. et al. Potential benefits of using radioactive ion beams for range margin reduction in carbon ion therapy. *Sci. Rep.* **12**, 21792 (2022).
90. Berthold, J. et al. Detectability of anatomical changes with prompt-gamma imaging: first systematic evaluation of clinical application during prostate-cancer proton therapy. *Int. J. Radiat. Oncol. Biol. Phys.* **117**, 718–729 (2023).
91. Hueso-González, F., Rabe, M., Ruggieri, T. A., Bortfeld, T. & Verburg, J. M. A full-scale clinical prototype for proton range verification using prompt gamma-ray spectroscopy. *Phys. Med. Biol.* **63**, 185019 (2018).
92. Kozani, M. K., Rucinski, A. & Moskal, P. J-PET application as a Compton camera for proton beam range verification: a preliminary study. *Bio-Algorithms Med-Syst.* **19**, 23–30 (2023).
93. Mattei, I. et al. Charged particles and neutron trackers: applications to particle therapy. *Nucl. Instrum. Methods Phys. Res. A* **954**, 161229 (2020).
94. Schauer, J. et al. Range verification of a clinical proton beam in an abdominal phantom by co-registration of ionoacoustics and ultrasound. *Phys. Med. Biol.* **68**, 125009 (2023).
95. Kim, K., Pandey, P. K., Gonzalez, G., Chen, Y. & Xiang, L. Simulation study of protoacoustics as a real-time in-line dosimetry tool for FLASH proton therapy. *Med. Phys.* **51**, 5070–5080 (2023).
96. Endo, K., Mishima, K., Fukumoto, S., Ninomiya, S. & Silvestrov, J. G. Table-top proton synchrotron ring for medical applications. In *Proc. EPAC 2000* (eds Mitaroff, W. A. et al.) 2515–2517 (JACoW Publishing, 2000).
97. Picardi, L. et al. Preliminary design of a very compact protosynchrotron for proton therapy. In *Proc. 4th European Particle Accelerator Conference* (eds Suller, V. P. & Petit-Jean-Genaz, C.) 2607–2609 (World Scientific, 1994).
98. Rossi, L. & Bottura, L. Superconducting magnets for particle accelerators. *Instrum. Exp. Tech.* **41**, 595–608 (1998).
99. Mizushima, K. et al. Concept design of a superconducting magnet for a compact heavy-ion synchrotron. *IEEE Trans. Appl. Supercond.* **32**, 4401405 (2022).
100. Peach, K. J. et al. Conceptual design of a nonscaling fixed field alternating gradient accelerator for protons and carbon ions for charged particle therapy. *Phys. Rev. Spec. Top. Accel. Beams* **16**, 030101 (2013).
101. Autin, B. et al. The FFAG R&D and medical application project RACCAM. *Proc. EPAC 2006* (eds Biscari, C. et al.) 2308–2309 (JACoW Publishing, 2006).
102. Garland, J. M., Appleby, R. B., Owen, H. & Tygier, S. Normal-conducting scaling fixed field alternating gradient accelerator for proton therapy. *Phys. Rev. Spec. Top. Accel. Beams* **18**, 094701 (2015).
103. Smirnov, V. L., Azaryan, N. S., Vorozhtsov, S. B. & Dzhelepov. *Preliminary Parameter Assessments of a Spiral FFAG Accelerator for Proton Therapy* (Dzhelepov Laboratory of Nuclear Problems, Joint Institute for Nuclear Research, 2013).
104. Degiovanni, A. & Amaldi, U. History of hadron therapy accelerators. *Phys. Med.* **31**, 322–332 (2015).
105. Ma, W. J. et al. Laser acceleration of highly energetic carbon ions using a double-layer target composed of slightly underdense plasma and ultrathin foil. *Phys. Rev. Lett.* **122**, 014803 (2019).
106. Linz, U. & Alonso, J. Laser-driven ion accelerators for tumor therapy revisited. *Phys. Rev. Accel. Beams* **19**, 124802 (2016).
107. Aymar, G. et al. LhARA: the laser-hybrid accelerator for radiobiological applications. *Front. Phys.* **8**, 567738 (2020).
108. Parodi, K. Imaging in radiotherapy. In *Proc. CAS-CERN Accelerator School on Accelerators for Medical Applications* Vol. 1 (ed. Bailey, R.) 75 (CERN, 2017).

Acknowledgements

V.M. acknowledges financial support from the Berry Foundation, Swiss National Science Foundation and Innosuisse funding scheme BRIDGE. B.C. acknowledges the support of NIH-NCI grants 1R37CA288343-01

and 1R03CA280213-01A1. M.S. acknowledges financial support to his department from the Kuni Foundation, Ion Beam Applications (IBA) and RaySearch Laboratories. E.S. acknowledges financial support from the US Department of Energy (DOE) under contract DE-AC02-76SF00515. K.P. acknowledges financial support from the European Commission (grant numbers 955956 and 883425), the German Research Foundation (DFG, grant numbers 372393016 and 441208898) and the One Munich Strategy Forum around the topics of positron-emission tomography and prompt gamma monitoring, as well as ion and photon counting imaging. M.D. acknowledges the support of ERC advanced grant 883425 (BARB) and EU Horizon2020 grant 101008548 (HITRIplus).

Competing interests
The authors declare no competing interests.

Additional information
Correspondence and requests for materials should be addressed to Vivek Maradia.

Peer review information *Nature Physics* thanks Boon-Keng Kevin Teo, Sonja Schellhammer and the other, anonymous, reviewer(s) for their contribution to the peer review of this work.